



Published in final edited form as:

ACS Comb Sci. 2012 December 10; 14(12): 680–687. doi:10.1021/co300111f.

## Systematic Evaluation of the Dependence of Deoxyribozyme Catalysis on Random Region Length

Tania E. Velez<sup>†</sup>, Jaydeep Singh<sup>†</sup>, Ying Xiao, Emily C. Allen, On Yi Wong, Madhavaiah Chandra, Sarah C. Kwon, and Scott K. Silverman<sup>\*</sup>

Department of Chemistry, University of Illinois at Urbana-Champaign, 600 South Mathews Avenue, Urbana, IL 61801, USA

### Abstract

Functional nucleic acids are DNA and RNA aptamers that bind targets, or they are deoxyribozymes and ribozymes that have catalytic activity. These functional DNA and RNA sequences can be identified from random-sequence pools by in vitro selection, which requires choosing the length of the random region. Shorter random regions allow more complete coverage of sequence space but may not permit the structural complexity necessary for binding or catalysis. In contrast, longer random regions are sampled incompletely but may allow adoption of more complicated structures that enable function. In this study, we systematically examined random region length ( $N_{20}$  through  $N_{60}$ ) for two particular deoxyribozyme catalytic activities, DNA cleavage and tyrosine-RNA nucleopeptide linkage formation. For both activities, we previously identified deoxyribozymes using only  $N_{40}$  regions. In the case of DNA cleavage, here we found that shorter  $N_{20}$  and  $N_{30}$  regions allowed robust catalytic function, either by DNA hydrolysis or by DNA deglycosylation and strand scission via  $\beta$ -elimination, whereas longer  $N_{50}$  and  $N_{60}$  regions did not lead to catalytically active DNA sequences. Follow-up selections with  $N_{20}$ ,  $N_{30}$ , and  $N_{40}$  regions revealed an interesting interplay of metal ion cofactors and random region length. Separately, for Tyr-RNA linkage formation,  $N_{30}$  and  $N_{60}$  regions provided catalytically active sequences, whereas  $N_{20}$  was unsuccessful, and the  $N_{40}$  deoxyribozymes were functionally superior (in terms of rate and yield) to  $N_{30}$  and  $N_{60}$ . Collectively, the results indicate that with future in vitro selection experiments for DNA and RNA catalysts, and by extension for aptamers, random region length should be an important experimental variable.

### INTRODUCTION

Naturally occurring RNA aptamers form key binding elements of riboswitches,<sup>1</sup> and natural RNA enzymes (ribozymes) catalyze RNA cleavage and ligation reactions<sup>2</sup> as well as peptide bond formation in the ribosome.<sup>3</sup> In contrast, natural DNA aptamers or enzymes (deoxyribozymes) have not been reported. The identification of the first natural ribozymes spurred searches for artificial aptamers and nucleic acid enzymes, comprising both RNA<sup>4–6</sup> and soon thereafter DNA.<sup>7–9</sup> Such searches are performed using in vitro selection, which is a powerful approach for identifying new, functional DNA or RNA sequences from random-

<sup>\*</sup>Corresponding Author: Phone: 217-244-4489. Fax: 217-244-8024. scott@scs.illinois.edu.

<sup>†</sup>T.E.V. and J.S. are co-first authors of this manuscript.

#### Notes

The authors declare no competing financial interest.

#### Supporting Information

Deoxyribozyme sequences, MALDI mass spectrometry data, and additional kinetic data. This material is available free of charge via the Internet at <http://pubs.acs.org>.

sequence “pools”.<sup>10,11</sup> Many artificial DNA and RNA aptamers<sup>12</sup> and enzymes<sup>13–16</sup> have been found using selection methodologies.

In nearly all selection experiments, the length  $n$  of the pool’s random region is fixed at the outset of the experiment. With only four standard nucleotide monomers, the size of sequence space increases as  $4^n$ . The physical sample of the initial pool is typically prepared by solid-phase synthesis for a DNA pool, or by transcription using a DNA template itself prepared by solid-phase synthesis for an RNA pool. As a practical limitation, the amount of the starting pool is on the order of  $10^{14}$  molecules (200 pmol), or perhaps  $10^{15}$  or  $10^{16}$  in some cases. In comparison, the  $4^n$  size of sequence space can be considerably larger; for example, for a 60-nucleotide  $N_{60}$  pool,  $4^{60} \approx 10^{36}$ . The sampling of sequence space is extremely sparse for long random regions. For the  $N_{60}$  case,  $10^{14}/10^{36} = 10^{-22}$  is the fraction of sequence space sampled. To the best of our knowledge, the longest reported random region is  $N_{228}$ , for which only  $10^{-123}$  of sequence space is covered.<sup>17</sup> Towards the other end of the length spectrum, an  $N_{20}$  region has only  $4^{20} = 10^{12}$  possible sequence permutations, and a typical starting pool with  $10^{14}$  molecules will sample essentially every possible 20-nucleotide sequence ( $10^2$  molecules of each  $N_{20}$  sequence, on average).

In any particular selection experiment, the choice of random region length  $n$  requires a compromise between two competing considerations: (1) coverage of sequence space, where shorter random regions allow greater coverage; and (2) potential structural complexity of the nucleic acid motifs, where longer random regions allow greater complexity of secondary and tertiary structure. Another consideration is that longer random regions may suffer from increased propensity to misfold, or from inhibition of catalytic portions by the excess sequence elements.<sup>18</sup> The choice of  $n$  is typically made in a relatively arbitrary fashion; some labs may prefer  $N_{40}$  pools, others  $N_{50}$ , and others  $N_{70}$ , and each lab rarely if ever uses one of the “other” lengths. Without experimentally assessing the emergent binding or catalysis as a systematic function of random region length, one cannot be confident in choosing the best compromise between sequence space coverage and structural complexity.

Theoretical calculations have explored the probabilities of finding various structural motifs in random-sequence pools,<sup>18–20</sup> among other sophisticated computational analyses of selection processes.<sup>21–25</sup> However, experiments are the ultimate arbiter of success in identifying ligands or catalysts. Only a small number of reports have strived to examine empirically the importance of random region length for a particular binding or catalytic activity. Huang et al. sought ribozymes for coenzyme synthesis by mixing pools of widely varying lengths ( $N_{30}$ ,  $N_{60}$ ,  $N_{100}$ , and  $N_{140}$ ), finding activity only from the  $N_{30}$  and  $N_{60}$  sequences.<sup>26,27</sup> However, under these competitive selection conditions, an additional consideration is the strong replicative advantage of shorter sequences, which is not an issue when different length pools are studied separately rather than competing directly.<sup>28</sup> Yarus and coworkers examined random regions from length 16 to 90 under noncompetitive conditions to identify RNA aptamers for the amino acid isoleucine, finding that 50 or 70 nt random regions were optimal.<sup>29</sup>

We are unaware of studies in which any kind of deoxyribozyme catalysis has been examined as a function of random region length. In the present study, we chose two particular catalytic activities for systematic analysis (Figure 1). First, we examined DNA-catalyzed DNA cleavage, where we have previously identified deoxyribozymes with rate enhancements  $>10^{13}$  for phosphodiester bond hydrolysis.<sup>30,31</sup> Second, we examined DNA-catalyzed nucleopeptide linkage formation, which we have identified as part of our larger efforts that seek DNA-catalyzed covalent modification of amino acid side chains.<sup>32–37</sup> For both types of catalytic activity, our previous efforts used only  $N_{40}$  random regions, where  $4^{40} \approx 10^{24}$  and therefore  $10^{14}/10^{24} = 10^{-10}$  of sequence space was explored. Here, for both kinds of

catalysis we examined  $N_{20}$  through  $N_{60}$  pools in new, independent selection experiments. For  $N_{20}$ , sequence space is fully covered, as noted above. For  $N_{30}$ ,  $N_{50}$ , and  $N_{60}$ , the fractions of covered sequence space are approximately  $10^{-4}$ ,  $10^{-16}$ , and  $10^{-22}$ , respectively. For both DNA-catalyzed reactions, the results showed that the length of the random region substantially impacts the outcome of the selection process, with important implications for future in vitro selection experiments.

## RESULTS AND DISCUSSION

### DNA-Catalyzed DNA Cleavage: Selection Experiments with $N_{20}$ through $N_{60}$ Random Regions

Our previous in vitro selection experiments to identify deoxyribozymes for DNA cleavage have used solely  $N_{40}$  random regions.<sup>30,31,38-40</sup> Here, we separately performed analogous experiments using  $N_{20}$ ,  $N_{30}$ ,  $N_{50}$ , and  $N_{60}$  pools. The selection process was performed using our previously described approach,<sup>31,41,42</sup> with a single-stranded DNA substrate and a deoxyribozyme that interacts with the substrate via two fixed Watson-Crick binding arms (Figure 1A). Each iterated selection round consisted of three steps of (1) PCR amplification of the population from the previous round, (2) enzymatic ligation of the DNA substrate to the amplified pool, and finally (3) incubation to allow individual active deoxyribozyme sequences to cleave their attached DNA substrate. Active deoxyribozyme sequences were separated by polyacrylamide gel electrophoresis (PAGE) on the basis of the downward shift due to loss of approximately half of the DNA substrate. During this key selection step, the incubation conditions were 70 mM HEPES, pH 7.5, 1 mM  $ZnCl_2$ , 20 mM  $MnCl_2$ , 40 mM  $MgCl_2$ , and 150 mM NaCl at 37 °C for 14 h. The resulting deoxyribozymes function without covalent attachment to the DNA substrate via the loop that is remote from the hydrolysis site.

After nine selection rounds, the  $N_{50}$  and  $N_{60}$  experiments showed no detectable activity (<0.2%) and were discontinued. In contrast, the  $N_{20}$  and  $N_{30}$  selections led to detectable (>0.2%) cleavage activity beginning at round 4 ( $N_{20}$ , 0.9%) and round 5 ( $N_{30}$ , 7.5%). Each pool was cloned from round 8 (48% and 45% for  $N_{20}$  and  $N_{30}$ , respectively), and individual deoxyribozymes were characterized (see sequences in Figure S1).

From the  $N_{20}$  pool, nine individual deoxyribozymes were obtained, exhibiting a range of cleavage sites along the DNA substrate (Figure 2A). The cleavage rate constant  $k_{obs}$  was as high as  $0.2\text{ h}^{-1}$  (Figure 3A and Figure S2A). MALDI mass spectrometry revealed that two of these nine  $N_{20}$  deoxyribozymes catalyze site-specific DNA phosphodiester hydrolysis, whereas seven catalyze deglycosylation followed by strand scission via two  $\beta$ -elimination reactions (Figure 4 and Tables S1 and S2). Both we<sup>40</sup> and others<sup>43</sup> have observed deglycosylation-induced DNA cleavage by unrelated deoxyribozymes. Similar results were found for the  $N_{30}$  pool, which led to 14 individual deoxyribozymes with a range of cleavage sites (Figure 2B). The cleavage  $k_{obs}$  was as high as  $0.5\text{ h}^{-1}$  (Figure 3B and Figure S2B). MALDI mass spectrometry indicated that three of these  $N_{30}$  deoxyribozymes hydrolyze the DNA substrate site-specifically, whereas 11 induce deglycosylation and strand scission (Figure 4 and Tables S1 and S2). Curiously, our selection experiments with  $N_{40}$  random regions led almost entirely to hydrolysis,<sup>31</sup> whereas the  $N_{20}$  and  $N_{30}$  selections described here led to many deoxyribozymes that catalyze deglycosylation and strand scission via  $\beta$ -elimination. This unexpected functional distinction between  $N_{20}/N_{30}$  and  $N_{40}$  selections highlights the importance of random region length as a variable that should be explored during selection experiments.

## DNA-Catalyzed DNA Hydrolysis: Follow-Up Experiments to Explore Interplay between Metal Ion Cofactors and Random Region Length

From the above-described efforts along with our previous work,<sup>30,31,38–40</sup> we inferred that the longer random-region lengths ( $N_{50}$  and  $N_{60}$ ) are sampled too sparsely for successful identification of deoxyribozymes that catalyze DNA cleavage, whereas  $N_{20}$ ,  $N_{30}$ , and  $N_{40}$  permit such identification. Excess sequence elements in the  $N_{50}$  and  $N_{60}$  sequences may also have suppressed the function of what otherwise would be active catalysts derived from shorter DNA segments. Whichever explanation applies, the outcome is that no activity was observed from the  $N_{50}$  and  $N_{60}$  pools, but the  $N_{20}$  and  $N_{30}$  (and  $N_{40}$ ) pools led to substantial catalytic function. We noted that the majority of the new  $N_{20}$  and  $N_{30}$  deoxyribozymes cleave their DNA substrate by a non-hydrolytic pathway, whereas hydrolysis is the more desirable outcome, e.g., for preparative purposes. We also considered that all of the prior and current selection experiments were performed with both  $Zn^{2+}$  and  $Mn^{2+}$  (as well as  $Mg^{2+}$ ) as available metal ion cofactors. In many cases, the outcome was that both  $Zn^{2+}$  and  $Mn^{2+}$  were required for catalysis, although one of our earlier ( $N_{40}$ ) DNA-hydrolyzing deoxyribozymes was subsequently shown to require only  $Zn^{2+}$ ,<sup>39</sup> as were several subsequently identified deoxyribozymes.<sup>40</sup>

We therefore performed a set of follow-up selection experiments, with two key changes to the procedure. First, we implemented a “capture step” immediately after each selection step, using T4 DNA ligase and a splinted 5′-phosphorylated donor oligonucleotide to capture the 3′-hydroxyl group uniquely revealed by DNA-catalyzed DNA hydrolysis (see Experimental Procedures) but not by deglycosylation, which after strand scission leads to a 3′-phosphate group. Selection pressure via a similar capture step was implemented in one of our previous reports (see Figure 5 in ref. 31, which depicts capture of the 5′-phosphate product as the selection pressure to achieve cleavage-site specificity). Second, in addition to including both  $Zn^{2+}/Mn^{2+}$  during the selection step, we separately evaluated providing  $Zn^{2+}$  alone as the divalent metal ion cofactor. Because we have already reported the outcome from evaluating  $N_{40}$  with  $Zn^{2+}/Mn^{2+}$ ,<sup>31</sup> here we performed five new follow-up selection experiments:  $N_{20}$  and  $N_{30}$  with  $Zn^{2+}/Mn^{2+}$ , and  $N_{20}$ ,  $N_{30}$ , and  $N_{40}$  with  $Zn^{2+}$  alone, all five now with inclusion of selection pressure via the capture step to enforce DNA-catalyzed DNA hydrolysis.

Of these five follow-up selection experiments, only the combination of  $N_{30}$  with  $Zn^{2+}$  and  $Mn^{2+}$  led to no activity through 12 selection rounds; this experiment was discontinued. The other four efforts all led to considerable catalytic activity, and each was cloned ( $N_{20}$  with  $Zn^{2+}$ : 26% at round 7;  $N_{20}$  with  $Zn^{2+}/Mn^{2+}$ : 4% at round 9;  $N_{30}$  with  $Zn^{2+}$ , 25% at round 7;  $N_{40}$  with  $Zn^{2+}$ , 12% at round 9). Each experiment led to just one or two distinct deoxyribozyme sequences (Figure S1), with  $k_{obs}$  as high as  $0.5\text{ h}^{-1}$  (Figure 5). MALDI mass spectrometry confirmed that all of these deoxyribozymes catalyze site-specific DNA hydrolysis at the expected location within the DNA substrate, with formation of 3′-hydroxyl and 5′-phosphate termini (Table S1). Non-hydrolytic cleavage via deglycosylation and strand scission was not observed by any of these deoxyribozymes, consistent with the stringent nature of the applied selection pressure. Notably, all five (out of five) of the  $N_{20}$  and  $N_{30}$  deoxyribozymes from these follow-up selection experiments led to DNA hydrolysis, whereas in the first set of  $N_{20}$  and  $N_{30}$  selections, only five out of 23 did so; clearly the selection pressure via the splint ligation capture step is highly effective.

All four of the new  $N_{20}/N_{30}/N_{40}$  DNA-hydrolyzing deoxyribozymes that were identified with  $Zn^{2+}$  alone were tested briefly for substrate sequence generality, by varying all DNA substrate nucleotides except for the unpaired C^G at the substrate cleavage site and covarying the deoxyribozyme binding arms to maintain Watson-Crick base pairing.<sup>31</sup> None of these four deoxyribozymes retained detectable (>0.2%) catalytic activity when the

substrate nucleotides were changed systematically in this fashion ( $A \leftrightarrow T$ ,  $G \leftrightarrow C$ ; data not shown). Because our previous  $N_{40}$  experiments with  $Zn^{2+}/Mn^{2+}$  did lead to numerous highly general DNA-hydrolyzing deoxyribozymes,<sup>31</sup> the present finding indicates that the use of  $Zn^{2+}$  alone as the cofactor comes at an apparent functional cost, namely the loss of tolerance for a range of DNA substrate sequences. We previously observed a similar compromise for our lone prior example of an  $N_{40}$  deoxyribozyme that is active with  $Zn^{2+}$  alone.<sup>38</sup>

We did not anticipate the experimental outcome that the shorter  $N_{20}$  and  $N_{30}$  pools lead to better catalysis with  $Zn^{2+}$  alone rather than with  $Zn^{2+}$  and  $Mn^{2+}$ . In Figure 5, note that 9ZH5 — identified with  $N_{20}$  and  $Zn^{2+}/Mn^{2+}$  — had the worst activity of all six new deoxyribozymes, and the  $N_{30}$  selection with  $Zn^{2+}/Mn^{2+}$  led to no activity at all. This finding highlights the relatively “rugged” nature of selection landscapes, in that changing the pool length from  $N_{40}$  to  $N_{20}/N_{30}$  unpredictably changed the optimal metal ions from  $Zn^{2+}$  and  $Mn^{2+}$  together to  $Zn^{2+}$  alone. These results establish an interesting interplay for DNA-catalyzed DNA hydrolysis between two key selection variables, random region length and divalent metal ion cofactors. A more general implication of these results is that one must be careful about assuming that a particular finding (e.g., with DNA hydrolysis and an  $N_{40}$  pool,  $Zn^{2+}/Mn^{2+}$  is superior to  $Zn^{2+}$  alone) will apply for different pool lengths (such as  $N_{20}$  and  $N_{30}$ ).

### DNA-Catalyzed Nucleopeptide Linkage Formation: Selection Experiments with $N_{20}$ – $N_{60}$ Random Regions

Separately from the above-described experiments with DNA-catalyzed DNA cleavage, we examined the influence of random region length on DNA-catalyzed nucleopeptide linkage formation, where all of our previous efforts with this reaction have been restricted to  $N_{40}$  random regions.<sup>32–36</sup> New selection experiments with  $N_{20}$ ,  $N_{30}$ , and  $N_{60}$  pools were performed as done previously,<sup>34</sup> using an “open” architecture and a Cys-Tyr-Ala tripeptide substrate connected via a flexible hexa(ethylene glycol) (HEG) tether to a DNA anchor oligonucleotide (Figure 1B). The electrophile for reaction with the tyrosine nucleophile was a 5′-triphosphorylated RNA strand. Iterated selection rounds were performed with incubation in 50 mM HEPES, pH 7.5, 20 mM  $MnCl_2$ , 40 mM  $MgCl_2$ , 150 mM NaCl and 2 mM KCl at 37 °C for 2 h in each key selection step. Active deoxyribozyme sequences were separated on the basis of their upward PAGE shift due to attachment of the RNA strand to the DNA-anchored Cys-Tyr-Ala tripeptide.

The impact of the random region length on the outcome of DNA-catalyzed nucleopeptide linkage formation was found to be very different from the observations with DNA-catalyzed DNA cleavage as described above. Here, the  $N_{20}$  pool led to no detectable activity after nine rounds and was discontinued. In contrast, both of the  $N_{30}$  and  $N_{60}$  pools led to substantial catalytic activity:  $N_{30}$  35% at round 8 and  $N_{60}$  26% at round 7. Each of these selection experiments was cloned, and individual deoxyribozymes were characterized further. From the  $N_{30}$  selection, a single distinct deoxyribozyme sequence was identified (Figure S1), with rate constant and yield substantially lower than those of the analogous  $N_{40}$  deoxyribozymes that were identified previously ( $k_{obs}$  0.15 h<sup>-1</sup> and 52% yield at 20 h for  $N_{30}$ , versus 0.95 h<sup>-1</sup> and 73% yield for  $N_{40}$ ; Figure 6).<sup>34</sup> From the  $N_{60}$  selection, two deoxyribozymes sequences were found (Figure S1), and their rate constants and yields were also considerably lower than for  $N_{40}$  ( $k_{obs}$  0.07 h<sup>-1</sup> and 19% yield for the more active variant; Figure 6). MALDI mass spectrometry confirmed that for all of these deoxyribozymes, the product was consistent with formation of the expected Tyr-RNA nucleopeptide linkage (Table S3). Therefore, for DNA-catalyzed nucleopeptide linkage formation, the outcomes with random region lengths other than  $N_{40}$  were markedly different than the outcomes for DNA-catalyzed DNA hydrolysis, in terms of both (i) which particular random region lengths led to observable catalytic activity, and (ii) quantitative aspects of the catalysis.

## General Implications of the Findings for Future In Vitro Selection Experiments

Most laboratories that perform in vitro selection appear to settle on using just one random region length. The specific choice of random region length is usually arbitrary or at least not specifically justified, except perhaps by reference to past successful selections using the same length. Our own laboratory has generally favored  $N_{40}$ , but without any systematic examination (until now) of shorter or longer random regions. Similarly, others typically use  $N_{60}$  or other lengths. We undertook the present study to provide discrete experimental data regarding impact of random region length on identification of DNA catalysts. The most important implication of our collective results is that one particular random region length is not optimal for all catalytic activities, and therefore the planning of in vitro selection experiments should prominently take into account “random region length” as an important experimental variable. This is a nontrivial consideration, given the wide range of other variables that may also be adjusted along with the reality that a finite number of selection experiments can be performed in parallel, as well as the practical reality that most reported in vitro selection efforts have used only one random region length within each study. We are currently making use of the present findings in several experiments underway in our laboratory, in which we are now systematically evaluating random region lengths other than our previously standard  $N_{40}$ . Although the results described here were obtained specifically in the context of DNA catalysts, we anticipate that they also apply to RNA catalysts as well as both DNA and RNA aptamers.

## EXPERIMENTAL PROCEDURES

### Oligonucleotide preparation

DNA oligonucleotides were prepared by solid-phase synthesis at Integrated DNA Technologies (Coralville, IA) and purified by denaturing 20% or 8% PAGE. To avoid chelation of  $Zn^{2+}$  by adventitious EDTA, all substrates and deoxyribozymes used in kinetic assays were extracted from gels using TN buffer (10 mM Tris, pH 8.0, 300 mM NaCl) lacking EDTA and precipitated with ethanol.

### In Vitro Selection for DNA-Catalyzed DNA Cleavage

In vitro selection for DNA-catalyzed DNA cleavage was performed essentially as described previously, using 200 pmol ( $\sim 10^{14}$  molecules) in each initial round of selection.<sup>31,41,42</sup>

For the initial selection experiments ( $N_{20}$ ,  $N_{30}$ ,  $N_{50}$ , and  $N_{60}$ , each with  $Zn^{2+}/Mn^{2+}/Mg^{2+}$ ), the deoxyribozyme pool strand was 5'-CGAAGTCGCCATCTCTTC- $N_x$ -ATAGTGAGTCGTATTAAGCTGATCCTGATGG-3', where the two underlined regions denote the substrate binding arms. The 5'-CGAA was replaced with 5'-CC and the 3'-terminus was ...TATTA-3' for individual deoxyribozymes prepared by solid-phase synthesis and used in the single-turnover in trans kinetic assays. The two PCR primers used during selection were 5'-CGAAGTCGCCATCTCTTC-3' (5'-phosphorylated to enable ligation by T4 RNA ligase) and 5'-(AAC)<sub>4</sub>XCCATCAGGATCAGCT-3' (where X denotes Glen Spacer 18, which is a PEG spacer that stops extension by Taq polymerase and leads to a size difference between the two PCR product strands). The DNA substrate used during selection was 5'-TAATACGACTCACTATCGAAGAGATGGCGACGGA-3', where the underlined C was unpaired and the three 3'-terminal nucleotides were RNA to enable ligation by T4 RNA ligase to the 5'-terminus of the deoxyribozyme pool strand. The DNA substrate for single-turnover in trans assays of individual deoxyribozymes was the all-DNA version of the substrate used during selection. The standard sample used in Figure 2 corresponds to hydrolysis immediately to the 5'-side of the unpaired C, with formation of 3'-hydroxyl and 5'-phosphate termini.

For the follow-up selection experiments ( $N_{20}$  and  $N_{30}$  each with either  $Zn^{2+}$  or  $Zn^{2+}/Mn^{2+}$ , or  $N_{40}$  with  $Zn^{2+}$ ), the deoxyribozyme pool strand and individual deoxyribozymes for kinetic assays were the same as in the first set of selection experiments. The two PCR primers used during selection were the same as in the first set of selection experiments, except the first primer was not 5'-phosphorylated. The DNA substrate used during selection and for single-turnover in trans kinetic assays of individual deoxyribozymes was 5'-GGATAATACGACTCACTATCGGAAGAGATGGCGACTTCG-3', where the underlined CG was unpaired. The 5'-phosphorylated terminus of the DNA substrate was joined to the 3'-terminus of the deoxyribozyme pool strand in each round of selection by splint ligation using T4 DNA ligase and a complementary DNA splint (5'-ATAGTGAGTCGTATTATCCTCCATCAGGATCAGCTTAATACGACTCACTAT-3'). The capture step in each selection round was performed by splint ligation essentially as described, using T4 DNA ligase.<sup>31</sup> The splint was 5'-ATCCTGATAACGAGAGGGCGATAGTGAGTCGTATTATCCTCCATCAGGATCAGCT-3', and the 5'-phosphorylated donor (to react with the 3'-OH group revealed after DNA hydrolysis) was 5'-GCCTCTCGTTATCAGGATAACAACAACAACAAC-3'.

### In Vitro Selection for DNA-Catalyzed Nucleopeptide Linkage Formation

In vitro selection for DNA-catalyzed nucleopeptide linkage formation was performed as described previously, using 200 pmol ( $\sim 10^{14}$  molecules) in each initial round of selection.<sup>34,41,42</sup> The deoxyribozyme pool strand was 5'-CGAAGTCGCCATCTCTTC-N<sub>x</sub>-ATAGTGAGTCGTATTAAGCTGATCCTGATGG-3', where the two underlined regions denote the substrate binding arms. The 5'-CGAA was replaced with 5'-CC and the 3'-terminus was ...TATTA-3' for individual deoxyribozymes prepared by solid-phase synthesis and used in the single-turnover in trans kinetic assays. The two PCR primers used during selection were 5'-CGAAGTCGCCATCTCTTC-3' (5'-phosphorylated to enable ligation by T4 RNA ligase) and 5'- $(AAC)_4$ XCCATCAGGATCAGCTTAATACGACTCACTAT-3' (where X denotes Glen Spacer 18). The RNA substrate used during selection was 5'-triphosphorylated 5'-GGAAGAGAUGGCGACGG-3', prepared by in vitro transcription using T7 RNA polymerase and a double stranded DNA template prepared by annealing two synthetic DNA oligonucleotides;<sup>44</sup> the 3'-terminus of the RNA substrate was joined by T4 RNA ligase to the 5'-terminus of the deoxyribozyme pool strand. The DNA-anchored tripeptide substrate was 5'-GGATAATACGACTCACTAT-3', joined via its 3'-terminus to a hexa(ethylene glycol) linker and the Cys-Tyr-Ala tripeptide through a disulfide bond as described.<sup>34</sup> The same DNA-anchored tripeptide substrate and 5'-triphosphorylated RNA substrate were used for single-turnover in trans kinetic assays of individual deoxyribozymes.

### DNA Cleavage Assays

The DNA cleavage assays were performed under single-turnover in trans conditions with the procedure described previously.<sup>38</sup> The DNA substrate was 5'-<sup>32</sup>P-radiolabeled using  $\gamma$ -<sup>32</sup>P-ATP and T4 polynucleotide kinase. The final incubation conditions were 70 mM HEPES, pH 7.5, 1 mM  $ZnCl_2$ , 20 mM  $MnCl_2$ , 40 mM  $MgCl_2$ , and 150 mM NaCl at 37 °C, with 10 nM DNA substrate and 1  $\mu$ M deoxyribozyme (1:100) in 20  $\mu$ L total volume. The  $Mn^{2+}$  and  $Mg^{2+}$  were omitted in some assays as indicated. Samples were separated by 20% PAGE and quantified with a PhosphorImager.

### Nucleopeptide Linkage Formation Assays

The nucleopeptide linkage formation assays were performed under single-turnover in trans conditions with the procedure described previously.<sup>34</sup> The DNA-anchored tripeptide substrate was 5'-<sup>32</sup>P-radiolabeled using  $\gamma$ -<sup>32</sup>P-ATP and T4 polynucleotide kinase. The final incubation conditions were 50 mM HEPES, pH 7.5, 20 mM  $MnCl_2$ , 40 mM  $MgCl_2$ , 150

mM NaCl, and 2 mM KCl at 37 °C, with 25 nM DNA-anchored tripeptide substrate, 0.5  $\mu$ M deoxyribozyme, and 1  $\mu$ M 5'-triphosphorylated RNA substrate (1:20:40) in 20  $\mu$ L total volume. Samples were separated by 20% PAGE and quantified with a PhosphorImager.

### MALDI mass spectrometry

Samples for MALDI mass spectrometry were prepared using the procedure described previously.<sup>30</sup> DNA cleavage samples were prepared using 100 pmol of DNA substrate and 200 pmol of deoxyribozyme in 50  $\mu$ L reaction volume. Nucleopeptide linkage formation samples for mass spectrometry were prepared using 500 pmol of DNA-anchored tripeptide substrate, 600 pmol of deoxyribozyme, and 800 pmol of 5'-triphosphorylated RNA substrate in 50  $\mu$ L reaction volume. All mass spectra were obtained in the mass spectrometry laboratory of the UIUC School of Chemical Sciences.

### Supplementary Material

Refer to Web version on PubMed Central for supplementary material.

### Acknowledgments

This research was supported by grants to S.K.S. from the National Institutes of Health (R01GM065966), the Defense Threat Reduction Agency (HDTRA1-09-1-0011), and the National Science Foundation (CHE0842534).

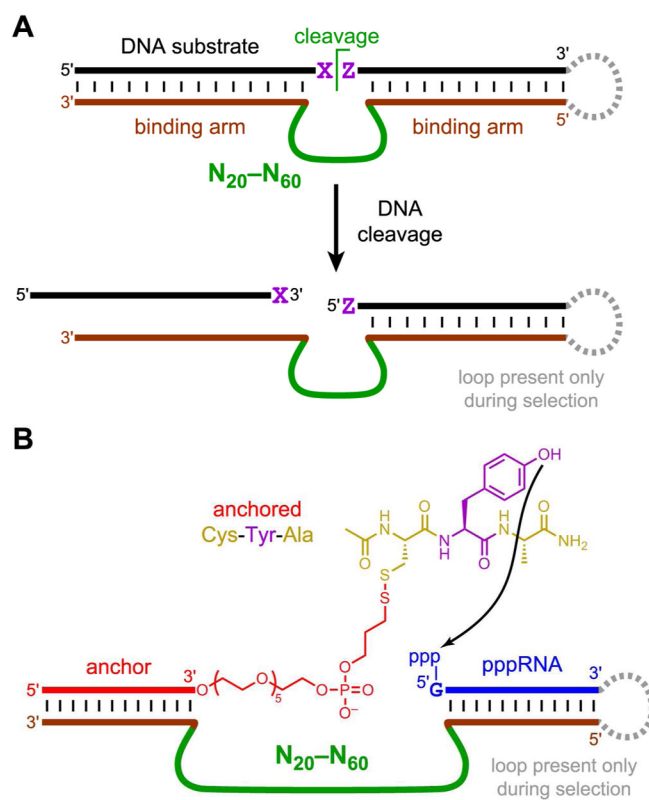
### References

1. Roth A, Breaker RR. The Structural and Functional Diversity of Metabolite-Binding Riboswitches. *Annu Rev Biochem.* 2009; 78:305–334. [PubMed: 19298181]
2. Doudna JA, Cech TR. The chemical repertoire of natural ribozymes. *Nature.* 2002; 418:222–228. [PubMed: 12110898]
3. Leung EK, Suslov N, Tuttle N, Sengupta R, Piccirilli JA. The mechanism of peptidyl transfer catalysis by the ribosome. *Annu Rev Biochem.* 2011; 80:527–555. [PubMed: 21548786]
4. Tuerk C, Gold L. Systematic evolution of ligands by exponential enrichment: RNA ligands to bacteriophage T4 DNA polymerase. *Science.* 1990; 249:505–510. [PubMed: 2200121]
5. Ellington AD, Szostak JW. In vitro selection of RNA molecules that bind specific ligands. *Nature.* 1990; 346:818–822. [PubMed: 1697402]
6. Robertson DL, Joyce GF. Selection in vitro of an RNA enzyme that specifically cleaves single-stranded DNA. *Nature.* 1990; 344:467–468. [PubMed: 1690861]
7. Ellington AD, Szostak JW. Selection in vitro of single-stranded DNA molecules that fold into specific ligand-binding structures. *Nature.* 1992; 355:850–852. [PubMed: 1538766]
8. Bock LC, Griffin LC, Latham JA, Vermaas EH, Toole JJ. Selection of single-stranded DNA molecules that bind and inhibit human thrombin. *Nature.* 1992; 355:564–566. [PubMed: 1741036]
9. Breaker RR, Joyce GF. A DNA enzyme that cleaves RNA. *Chem Biol.* 1994; 1:223–229. [PubMed: 9383394]
10. Joyce GF. Directed Evolution of Nucleic Acid Enzymes. *Annu Rev Biochem.* 2004; 73:791–836. [PubMed: 15189159]
11. Joyce GF. Forty Years of In Vitro Evolution. *Angew Chem Int Ed.* 2007; 46:6420–6436.
12. Silverman, SK. Artificial Functional Nucleic Acids: Aptamers, Ribozymes, and Deoxyribozymes Identified by In Vitro Selection. In: Li, Y.; Lu, Y., editors. *Functional Nucleic Acids for Analytical Applications.* Springer Science + Business Media, LLC; New York: 2009. p. 47-108.
13. Silverman SK. Catalytic DNA (deoxyribozymes) for synthetic applications—current abilities and future prospects. *Chem Commun.* 2008:3467–3485.
14. Schlosser K, Li Y. Biologically inspired synthetic enzymes made from DNA. *Chem Biol.* 2009; 16:311–322. [PubMed: 19318212]

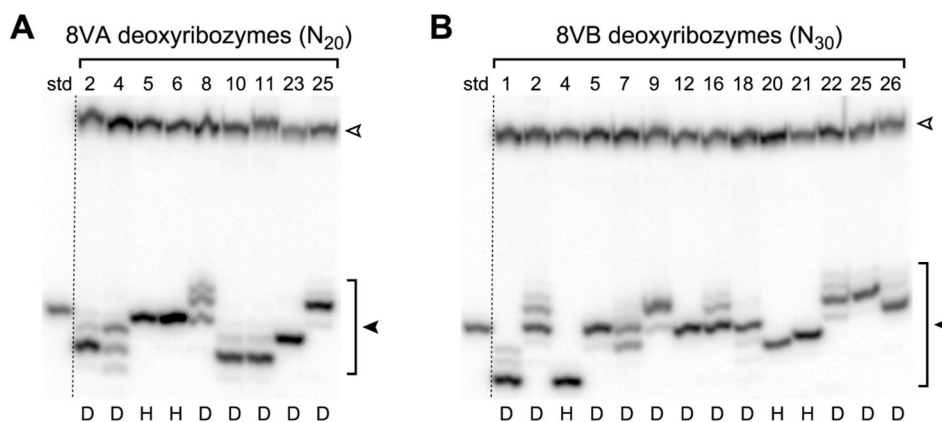


15. Silverman SK. DNA as a Versatile Chemical Component for Catalysis, Encoding, and Stereocontrol. *Angew Chem Int Ed.* 2010; 49:7180–7201.
16. Silverman, SK. In Vitro Selection and Application of Nucleic Acid Enzymes (Ribozymes and Deoxyribozymes). In: Begley, TP., editor. *Wiley Encyclopedia of Chemical Biology.* John Wiley and Sons; Hoboken, NJ: 2009.
17. Li Y, Geyer CR, Sen D. Recognition of anionic porphyrins by DNA aptamers. *Biochemistry.* 1996; 35:6911–6922. [PubMed: 8639643]
18. Sabeti PC, Unrau PJ, Bartel DP. Accessing rare activities from random RNA sequences: the importance of the length of molecules in the starting pool. *Chem Biol.* 1997; 4:767–774. [PubMed: 9375255]
19. Irvine D, Tuerk C, Gold L. SELEXION. Systematic evolution of ligands by exponential enrichment with integrated optimization by non-linear analysis. *J Mol Biol.* 1991; 222:739–761. [PubMed: 1721092]
20. Knight R, De Sterck H, Markel R, Smit S, Oshmyansky A, Yarus M. Abundance of correctly folded RNA motifs in sequence space, calculated on computational grids. *Nucleic Acids Res.* 2005; 33:5924–5935. [PubMed: 16237127]
21. Sun F, Galas D, Waterman MS. A mathematical analysis of in vitro molecular selection-amplification. *J Mol Biol.* 1996; 258:650–660. [PubMed: 8636999]
22. Gevertz J, Gan HH, Schlick T. In vitro RNA random pools are not structurally diverse: a computational analysis. *RNA.* 2005; 11:853–863. [PubMed: 15923372]
23. Levine HA, Nilsen-Hamilton M. A mathematical analysis of SELEX. *Comput Biol Chem.* 2007; 31:11–35. [PubMed: 17218151]
24. Chushak Y, Stone MO. In silico selection of RNA aptamers. *Nucleic Acids Res.* 2009; 37:e87. [PubMed: 19465396]
25. Kim N, Izzo JA, Elmetwaly S, Gan HH, Schlick T. Computational generation and screening of RNA motifs in large nucleotide sequence pools. *Nucleic Acids Res.* 2010; 38:e139. [PubMed: 20448026]
26. Huang F, Bugg CW, Yarus M. RNA-Catalyzed CoA, NAD, and FAD synthesis from phosphopantetheine, NMN, and FMN. *Biochemistry.* 2000; 39:15548–15555. [PubMed: 11112541]
27. Coleman TM, Huang F. RNA-catalyzed thioester synthesis. *Chem Biol.* 2002; 9:1227–1236. [PubMed: 12445773]
28. Coleman TM, Huang F. Optimal Random Libraries for the Isolation of Catalytic RNA. *RNA Biol.* 2005; 2:129–136. [PubMed: 17114928]
29. Legiewicz M, Lozupone C, Knight R, Yarus M. Size, constant sequences, and optimal selection. *RNA.* 2005; 11:1701–1709. [PubMed: 16177137]
30. Chandra M, Sachdeva A, Silverman SK. DNA-catalyzed sequence-specific hydrolysis of DNA. *Nature Chem Biol.* 2009; 5:718–720. [PubMed: 19684594]
31. Xiao Y, Wehrmann RJ, Ibrahim NA, Silverman SK. Establishing Broad Generality of DNA Catalysts for Site-Specific Hydrolysis of Single-Stranded DNA. *Nucleic Acids Res.* 2012; 40:1778–1786. [PubMed: 22021383]
32. Pradeepkumar PI, Höbartner C, Baum DA, Silverman SK. DNA-Catalyzed Formation of Nucleopeptide Linkages. *Angew Chem Int Ed.* 2008; 47:1753–1757.
33. Sachdeva A, Silverman SK. DNA-Catalyzed Serine Side Chain Reactivity and Selectivity. *Chem Commun.* 2010; 46:2215–2217.
34. Wong OY, Pradeepkumar PI, Silverman SK. DNA-Catalyzed Covalent Modification of Amino Acid Side Chains in Tethered and Free Peptide Substrates. *Biochemistry.* 2011; 50:4741–4749. [PubMed: 21510668]
35. Wong OY, Mulcrone AE, Silverman SK. DNA-Catalyzed Reductive Amination. *Angew Chem Int Ed.* 2011; 50:11679–11684.
36. Sachdeva A, Silverman SK. DNA-catalyzed reactivity of a phosphoramidate functional group and formation of an unusual pyrophosphoramidate linkage. *Org Biomol Chem.* 2012; 10:122–125. [PubMed: 22042295]

37. Sachdeva A, Chandra M, Chandrasekar J, Silverman SK. Covalent Tagging of Phosphorylated Peptides By Phosphate-Specific Deoxyribozymes. *Chem Bio Chem*. 2012; 13:654–657.
38. Xiao Y, Chandra M, Silverman SK. Functional Compromises among pH Tolerance, Site Specificity, and Sequence Tolerance for a DNA-Hydrolyzing Deoxyribozyme. *Biochemistry*. 2010; 49:9630–9637. [PubMed: 20923239]
39. Xiao Y, Allen EC, Silverman SK. Merely two mutations switch a DNA-hydrolyzing deoxyribozyme from heterobimetallic ( $Zn^{2+}/Mn^{2+}$ ) to monometallic ( $Zn^{2+}$ -only) behavior. *Chem Commun*. 2011; 47:1749–1751.
40. Dokukin V, Silverman SK. Lanthanide Ions as Required Cofactors for DNA Catalysts. *Chem Sci*. 2012; 3:1707–1714.
41. Flynn-Charlebois A, Wang Y, Prior TK, Rashid I, Hoadley KA, Coppins RL, Wolf AC, Silverman SK. Deoxyribozymes with 2'-5' RNA Ligase Activity. *J Am Chem Soc*. 2003; 125:2444–2454. [PubMed: 12603132]
42. Kost DM, Gerdt JP, Pradeepkumar PI, Silverman SK. Controlling regioselectivity and site-selectivity in RNA ligation by  $Zn^{2+}$ -dependent deoxyribozymes that use 2',3'-cyclic phosphate RNA substrates. *Org Biomol Chem*. 2008; 6:4391–4398. [PubMed: 19005599]
43. Sheppard TL, Ordoukhanian P, Joyce GF. A DNA enzyme with *N*-glycosylase activity. *Proc Natl Acad Sci USA*. 2000; 97:7802–7807. [PubMed: 10884411]
44. Milligan JF, Groebe DR, Witherell GW, Uhlenbeck OC. Oligoribonucleotide synthesis using T7 RNA polymerase and synthetic DNA templates. *Nucleic Acids Res*. 1987; 15:8783–8798. [PubMed: 3684574]

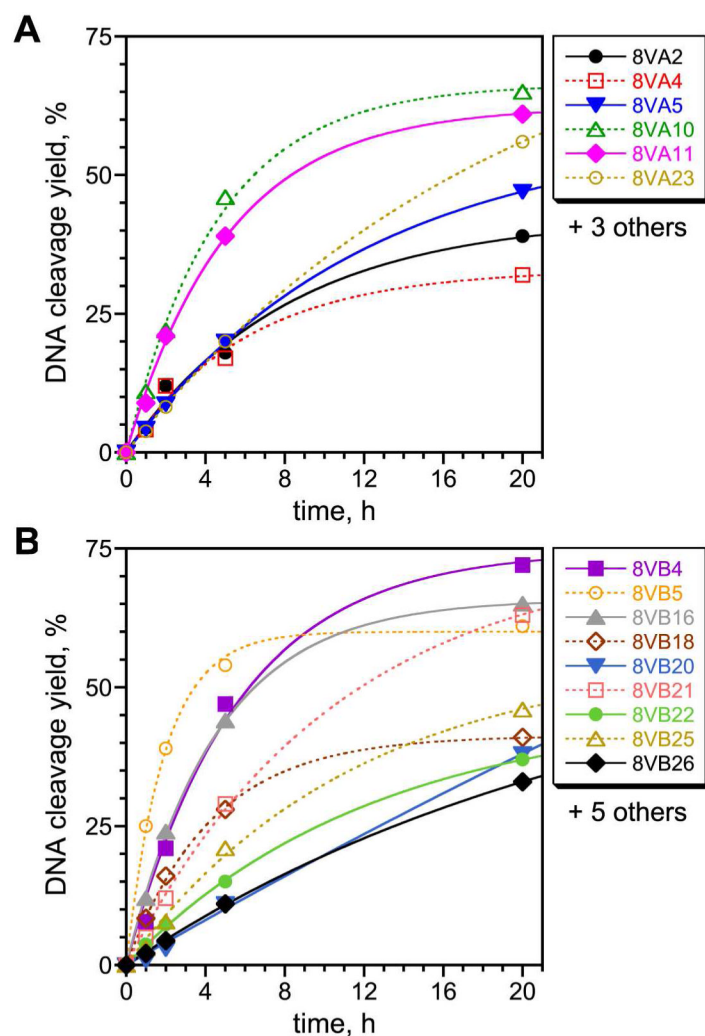


**Figure 1.** Two reactions systematically examined for the effect of random region length on DNA catalysis. In each case, the key selection step is illustrated. (A) DNA-catalyzed DNA cleavage. (B) DNA-catalyzed tyrosine-RNA nucleopeptide linkage formation.

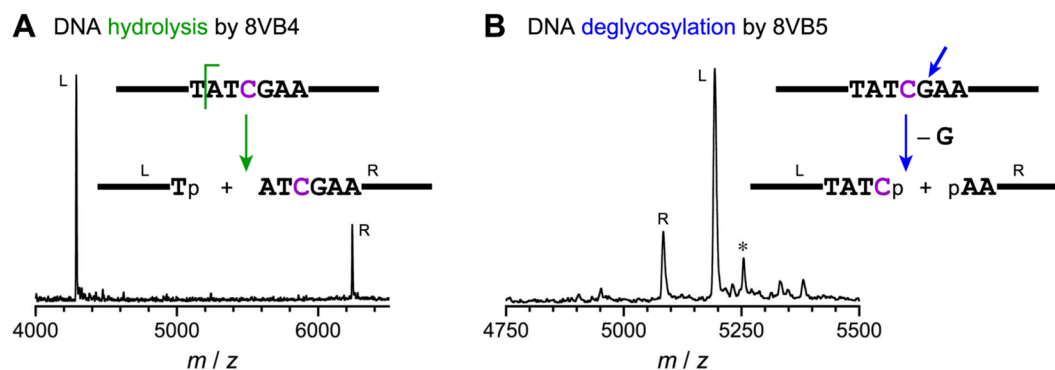


**Figure 2.**

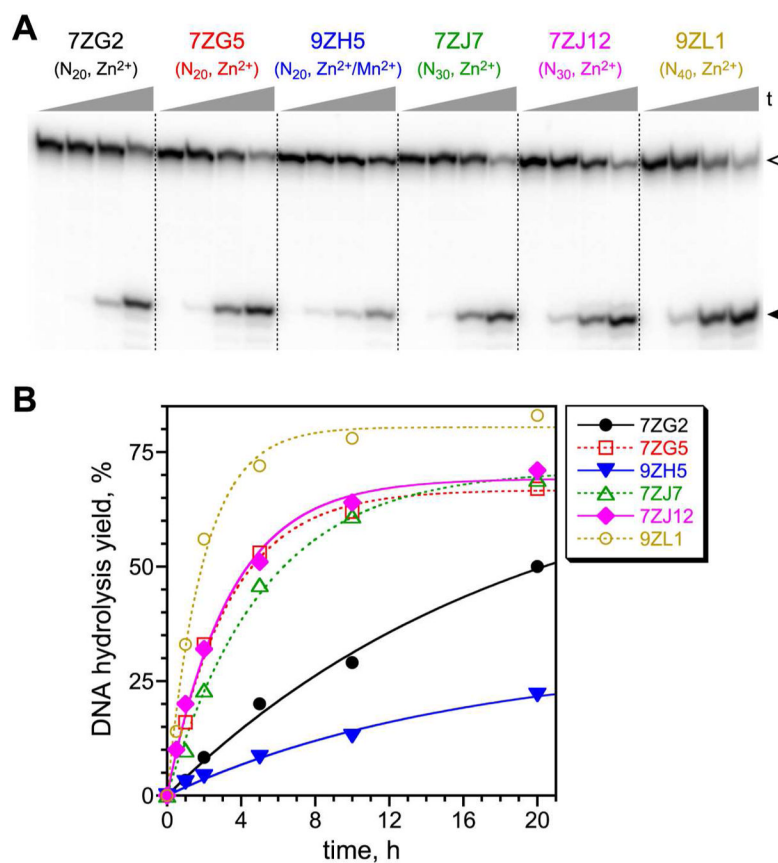
Various substrate cleavage sites for deoxyribozymes from the initial (A) N<sub>20</sub> and (B) N<sub>30</sub> selections for DNA-catalyzed DNA cleavage. Individual deoxyribozymes are denoted 8VA followed by a clone number for N<sub>20</sub> and 8VB followed by a clone number for N<sub>30</sub>. Each deoxyribozyme was allowed to cleave the 5'-<sup>32</sup>P-radiolabeled DNA substrate (*open arrowhead*), resulting in a product band (*filled arrowhead*) whose PAGE migration rate relative to the standard suggests the cleavage site. The standard sample corresponds to hydrolysis of the substrate sequence at the position noted in the Experimental Procedures. Incubation conditions: 70 mM HEPES, pH 7.5, 1 mM ZnCl<sub>2</sub>, 20 mM MnCl<sub>2</sub>, 40 mM MgCl<sub>2</sub>, and 150 mM NaCl at 37 °C (t = 20 h). Quantification of cleavage kinetics for each deoxyribozyme is provided in Figure 3. The reaction type (i.e., substrate hydrolysis, or substrate deglycosylation followed by two β-eliminations) and precise site of each cleavage reaction was assigned with confidence for each deoxyribozyme by MALDI mass spectrometry of the products (Figure 4; see Tables S1 and S2 for all data values and cleavage-site assignments). The type of reaction catalyzed by each deoxyribozyme is marked below its lane with “H” for hydrolysis or “D” for deglycosylation.



**Figure 3.** Kinetic plots for individual deoxyribozymes from the (A) N<sub>20</sub> and (B) N<sub>30</sub> selections for DNA cleavage. Kinetic plots for several additional deoxyribozymes from each selection experiment are shown in Figure S2.  $k_{\text{obs}}$  values are tabulated in Table S4. Incubation conditions as in Figure 2.

**Figure 4.**

Representative MALDI mass spectra to assign cleavage reactions and sites for deoxyribozymes from the initial  $N_{20}$  and  $N_{30}$  selections for DNA cleavage. All mass spectra data and precise cleavage-site assignments are tabulated in Tables S1 and S2. The indicated C nucleotide of the substrate was not base-paired with either deoxyribozyme binding arm (see Figure 1). (A) 8VB4 deoxyribozyme, which hydrolyzes the DNA substrate at a specific phosphodiester linkage and forms 3'-phosphate and 5'-hydroxyl products. Some of the new DNA-hydrolyzing deoxyribozymes lead instead to 3'-hydroxyl and 5'-phosphate products. (B) 8VB5 deoxyribozyme, which deglycosylates the DNA substrate at a specific guanosine. After two subsequent  $\beta$ -elimination reactions, the products are missing the entire G nucleoside and have 3'-phosphate and 5'-phosphate groups. Some of the new DNA-deglycosylating deoxyribozymes are not site-specific and deglycosylate the substrate at either of two adjacent nucleotide positions. In the spectrum of panel B, the asterisk denotes the peak for uncleaved substrate with  $z = 2$ .

**Figure 5.**

Activities of deoxyribozymes from the follow-up  $N_{20}$ ,  $N_{30}$ , and  $N_{40}$  selections for DNA-catalyzed DNA hydrolysis. (A) PAGE image for each of the six new deoxyribozymes, showing representative timepoints ( $t = 30$  s, 15 min, 2 h, and 20 h). Substrate (*open arrowhead*) and product (*filled arrowhead*) are marked. Incubation conditions: 70 mM HEPES, pH 7.5, 1 mM  $ZnCl_2$ , 20 mM  $MnCl_2$  if indicated, and 150 mM NaCl at 37 °C. (B) Kinetic plots.  $k_{obs}$  values are tabulated in Table S4.

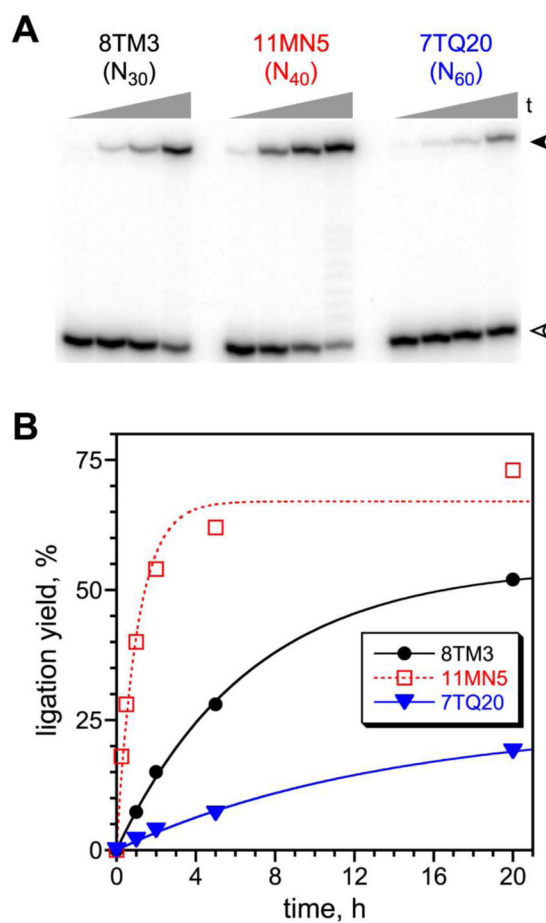


**Figure 6.**

Activities of deoxyribozymes from the selections for DNA-catalyzed nucleopeptide linkage formation. (A) PAGE image showing representative timepoints ( $t = 30$  s, 30 min, 2 h, and 20 h). Incubation conditions: 50 mM HEPES, pH 7.5, 20 mM  $\text{MnCl}_2$ , 40 mM  $\text{MgCl}_2$ , 150 mM NaCl, and 2 mM KCl at 37 °C. Substrate (*open arrowhead*) and product (*filled arrowhead*) are marked. For  $N_{30}$ , 8TM3 was the only new deoxyribozyme identified, along with two closely related sequence variants. For  $N_{40}$ , 11MN5 was the best deoxyribozyme identified previously by direct selection;<sup>31</sup> data shown here were newly acquired for comparison. For  $N_{60}$ , 7TQ20 was one of two different deoxyribozymes found, along with six close sequence variants; the other deoxyribozyme, 7TQ46 (no variants found), had slightly lower activity. (B) Kinetic plots.  $k_{\text{obs}}$  values are tabulated in Table S4.